EUROPEAN LABORATORY FOR PARTICLE PHYSICS

CERN-PPE/97-159
16th December 1997

Measurements of the B_s^0 and Λ_b^0 Lifetimes

The OPAL Collaboration

Abstract

This paper presents updated measurements of the lifetimes of the B_s^0 meson and the Λ_b^0 baryon using 4.4 million hadronic Z^0 decays recorded by the OPAL detector at LEP from 1990 to 1995. A sample of B_s^0 decays is obtained using $D_s^- \ell^+$ combinations, where the D_s^- is fully reconstructed in the $\phi\pi^-$, $K^{*0}K^-$ and $K^-K_S^0$ decay channels and partially reconstructed in the $\phi\ell^-\bar{\nu}X$ decay mode. A sample of Λ_b^0 decays is obtained using $\Lambda_c^+ \ell^-$ combinations, where the Λ_c^+ is fully reconstructed in its decay to a $pK^-\pi^+$ final state and partially reconstructed in the $\Lambda\ell^+\nu X$ decay channel. From 172 ± 28 $D_s^- \ell^+$ combinations attributed to B_s^0 decays, the measured lifetime is

$$\tau(B_s^0) = 1.50^{+0.16}_{-0.15} \pm 0.04\,\mathrm{ps},$$

where the errors are statistical and systematic, respectively. From the 129 ± 25 $\Lambda_c^+ \ell^-$ combinations attributed to Λ_b^0 decays, the measured lifetime is

$$\tau(\Lambda_b^0) = 1.29^{+0.24}_{-0.22} \pm 0.06\,\mathrm{ps},$$

where the errors are statistical and systematic, respectively.

(Submitted to Physics Letters)

The OPAL Collaboration

K. Ackerstaff[8], G. Alexander[23], J. Allison[16], N. Altekamp[5], K.J. Anderson[9], S. Anderson[12], S. Arcelli[2], S. Asai[24], S.F. Ashby[1], D. Axen[29], G. Azuelos[18,a], A.H. Ball[17], E. Barberio[8], R.J. Barlow[16], R. Bartoldus[3], J.R. Batley[5], S. Baumann[3], J. Bechtluft[14], C. Beeston[16], T. Behnke[8], A.N. Bell[1], K.W. Bell[20], G. Bella[23], S. Bentvelsen[8], S. Bethke[14], S. Betts[15], O. Biebel[14], A. Biguzzi[5], S.D. Bird[16], V. Blobel[27], I.J. Bloodworth[1], J.E. Bloomer[1], M. Bobinski[10], P. Bock[11], D. Bonacorsi[2], M. Boutemeur[34], S. Braibant[8], L. Brigliadori[2], R.M. Brown[20], H.J. Burckhart[8], C. Burgard[8], R. Bürgin[10], P. Capiluppi[2], R.K. Carnegie[6], A.A. Carter[13], J.R. Carter[5], C.Y. Chang[17], D.G. Charlton[1,b], D. Chrisman[4], P.E.L. Clarke[15], I. Cohen[23], J.E. Conboy[15], O.C. Cooke[8], C. Couyoumtzelis[13], R.L. Coxe[9], M. Cuffiani[2], S. Dado[22], C. Dallapiccola[17], G.M. Dallavalle[2], R. Davis[30], S. De Jong[12], L.A. del Pozo[4], K. Desch[3], B. Dienes[33,d], M.S. Dixit[7], M. Doucet[18], E. Duchovni[26], G. Duckeck[34], I.P. Duerdoth[16], D. Eatough[16], J.E.G. Edwards[16], P.G. Estabrooks[6], H.G. Evans[9], M. Evans[13], F. Fabbri[2], A. Fanfani[2], M. Fanti[2], A.A. Faust[30], L. Feld[8], F. Fiedler[27], M. Fierro[2], H.M. Fischer[3], I. Fleck[8], R. Folman[26], D.G. Fong[17], M. Foucher[17], A. Fürtjes[8], D.I. Futyan[16], P. Gagnon[7], J.W. Gary[4], J. Gascon[18], S.M. Gascon-Shotkin[17], N.I. Geddes[20], C. Geich-Gimbel[3], T. Geralis[20], G. Giacomelli[2], P. Giacomelli[4], R. Giacomelli[2], V. Gibson[5], W.R. Gibson[13], D.M. Gingrich[30,a], D. Glenzinski[9], J. Goldberg[22], M.J. Goodrick[5], W. Gorn[4], C. Grandi[2], E. Gross[26], J. Grunhaus[23], M. Gruwé[8], C. Hajdu[32], G.G. Hanson[12], M. Hansroul[8], M. Hapke[13], C.K. Hargrove[7], P.A. Hart[9], C. Hartmann[3], M. Hauschild[8], C.M. Hawkes[5], R. Hawkings[27], R.J. Hemingway[6], M. Herndon[17], G. Herten[10], R.D. Heuer[8], M.D. Hildreth[8], J.C. Hill[5], S.J. Hillier[1], P.R. Hobson[25], A. Hocker[9], R.J. Homer[1], A.K. Honma[28,a], D. Horváth[32,c], K.R. Hossain[30], R. Howard[29], P. Hüntemeyer[27], D.E. Hutchcroft[5], P. Igo-Kemenes[11], D.C. Imrie[25], M.R. Ingram[16], K. Ishii[24], A. Jawahery[17], P.W. Jeffreys[20], H. Jeremie[18], M. Jimack[1], A. Joly[18], C.R. Jones[5], G. Jones[16], M. Jones[6], U. Jost[11], P. Jovanovic[1], T.R. Junk[8], J. Kanzaki[24], D. Karlen[6], V. Kartvelishvili[16], K. Kawagoe[24], T. Kawamoto[24], P.I. Kayal[30], R.K. Keeler[28], R.G. Kellogg[17], B.W. Kennedy[20], J. Kirk[29], A. Klier[26], S. Kluth[8], T. Kobayashi[24], M. Kobel[10], D.S. Koetke[6], T.P. Kokott[3], M. Kolrep[10], S. Komamiya[24], T. Kress[11], P. Krieger[6], J. von Krogh[11], P. Kyberd[13], G.D. Lafferty[16], R. Lahmann[17], W.P. Lai[19], D. Lanske[14], J. Lauber[15], S.R. Lautenschlager[31], J.G. Layter[4], D. Lazic[22], A.M. Lee[31], E. Lefebvre[18], D. Lellouch[26], J. Letts[12], L. Levinson[26], S.L. Lloyd[13], F.K. Loebinger[16], G.D. Long[28], M.J. Losty[7], J. Ludwig[10], D. Lui[12], A. Macchiolo[2], A. Macpherson[30], M. Mannelli[8], S. Marcellini[2], C. Markopoulos[13], C. Markus[3], A.J. Martin[13], J.P. Martin[18], G. Martinez[17], T. Mashimo[24], P. Mättig[26], W.J. McDonald[30], J. McKenna[29], E.A. Mckigney[15], T.J. McMahon[1], R.A. McPherson[8], F. Meijers[8], S. Menke[3], F.S. Merritt[9], H. Mes[7], J. Meyer[27], A. Michelini[2], G. Mikenberg[26], D.J. Miller[15], A. Mincer[22,e], R. Mir[26], W. Mohr[10], A. Montanari[2], T. Mori[24], U. Müller[3], S. Mihara[24], K. Nagai[26], I. Nakamura[24], H.A. Neal[8], B. Nellen[3], R. Nisius[8], S.W. O'Neale[1], F.G. Oakham[7], F. Odorici[2], H.O. Ogren[12], A. Oh[27], N.J. Oldershaw[16], M.J. Oreglia[9], S. Orito[24], J. Pálinkás[33,d], G. Pásztor[32], J.R. Pater[16], G.N. Patrick[20], J. Patt[10], R. Perez-Ochoa[8], S. Petzold[27], P. Pfeifenschneider[14], J.E. Pilcher[9], J. Pinfold[30], D.E. Plane[8], P. Poffenberger[28], B. Poli[2], A. Posthaus[3], C. Rembser[8], S. Robertson[28], S.A. Robins[22], N. Rodning[30], J.M. Roney[28], A. Rooke[15], A.M. Rossi[2], P. Routenburg[30], Y. Rozen[22], K. Runge[10], O. Runolfsson[8], U. Ruppel[14], D.R. Rust[12], R. Rylko[25], K. Sachs[10], T. Saeki[24], W.M. Sang[25], E.K.G. Sarkisyan[23], C. Sbarra[29], A.D. Schaile[34], O. Schaile[34], F. Scharf[3], P. Scharff-Hansen[8], J. Schieck[11], P. Schleper[11], B. Schmitt[8], S. Schmitt[11], A. Schöning[8], M. Schröder[8], H.C. Schultz-Coulon[10], M. Schumacher[3], C. Schwick[8], W.G. Scott[20], T.G. Shears[16], B.C. Shen[4], C.H. Shepherd-Themistocleous[8], P. Sherwood[15], G.P. Siroli[2], A. Sittler[27], A. Skillman[15], A. Skuja[17], A.M. Smith[8], G.A. Snow[17], R. Sobie[28], S. Söldner-Rembold[10], R.W. Springer[30], M. Sproston[20], K. Stephens[16], J. Steuerer[27], B. Stockhausen[3], K. Stoll[10], D. Strom[19], R. Ströhmer[34], P. Szymanski[20], R. Tafirout[18], S.D. Talbot[1], S. Tanaka[24], P. Taras[18], S. Tarem[22], R. Teuscher[8], M. Thiergen[10], M.A. Thomson[8], E. von Törne[3], E. Torrence[8], S. Towers[6], I. Trigger[18], Z. Trócsányi[33], E. Tsur[23], A.S. Turcot[9], M.F. Turner-Watson[8], P. Utzat[11],

R. Van Kooten[12], M. Verzocchi[10], P. Vikas[18], E.H. Vokurka[16], H. Voss[3], F. Wäckerle[10], A. Wagner[27], C.P. Ward[5], D.R. Ward[5], P.M. Watkins[1], A.T. Watson[1], N.K. Watson[1], P.S. Wells[8], N. Wermes[3], J.S. White[28], B. Wilkens[10], G.W. Wilson[27], J.A. Wilson[1], T.R. Wyatt[16], S. Yamashita[24], G. Yekutieli[26], V. Zacek[18], D. Zer-Zion[8]

[1]School of Physics and Astronomy, University of Birmingham, Birmingham B15 2TT, UK
[2]Dipartimento di Fisica dell' Università di Bologna and INFN, I-40126 Bologna, Italy
[3]Physikalisches Institut, Universität Bonn, D-53115 Bonn, Germany
[4]Department of Physics, University of California, Riverside CA 92521, USA
[5]Cavendish Laboratory, Cambridge CB3 0HE, UK
[6]Ottawa-Carleton Institute for Physics, Department of Physics, Carleton University, Ottawa, Ontario K1S 5B6, Canada
[7]Centre for Research in Particle Physics, Carleton University, Ottawa, Ontario K1S 5B6, Canada
[8]CERN, European Organisation for Particle Physics, CH-1211 Geneva 23, Switzerland
[9]Enrico Fermi Institute and Department of Physics, University of Chicago, Chicago IL 60637, USA
[10]Fakultät für Physik, Albert Ludwigs Universität, D-79104 Freiburg, Germany
[11]Physikalisches Institut, Universität Heidelberg, D-69120 Heidelberg, Germany
[12]Indiana University, Department of Physics, Swain Hall West 117, Bloomington IN 47405, USA
[13]Queen Mary and Westfield College, University of London, London E1 4NS, UK
[14]Technische Hochschule Aachen, III Physikalisches Institut, Sommerfeldstrasse 26-28, D-52056 Aachen, Germany
[15]University College London, London WC1E 6BT, UK
[16]Department of Physics, Schuster Laboratory, The University, Manchester M13 9PL, UK
[17]Department of Physics, University of Maryland, College Park, MD 20742, USA
[18]Laboratoire de Physique Nucléaire, Université de Montréal, Montréal, Quebec H3C 3J7, Canada
[19]University of Oregon, Department of Physics, Eugene OR 97403, USA
[20]Rutherford Appleton Laboratory, Chilton, Didcot, Oxfordshire OX11 0QX, UK
[22]Department of Physics, Technion-Israel Institute of Technology, Haifa 32000, Israel
[23]Department of Physics and Astronomy, Tel Aviv University, Tel Aviv 69978, Israel
[24]International Centre for Elementary Particle Physics and Department of Physics, University of Tokyo, Tokyo 113, and Kobe University, Kobe 657, Japan
[25]Brunel University, Uxbridge, Middlesex UB8 3PH, UK
[26]Particle Physics Department, Weizmann Institute of Science, Rehovot 76100, Israel
[27]Universität Hamburg/DESY, II Institut für Experimental Physik, Notkestrasse 85, D-22607 Hamburg, Germany
[28]University of Victoria, Department of Physics, P O Box 3055, Victoria BC V8W 3P6, Canada
[29]University of British Columbia, Department of Physics, Vancouver BC V6T 1Z1, Canada
[30]University of Alberta, Department of Physics, Edmonton AB T6G 2J1, Canada
[31]Duke University, Dept of Physics, Durham, NC 27708-0305, USA
[32]Research Institute for Particle and Nuclear Physics, H-1525 Budapest, P O Box 49, Hungary
[33]Institute of Nuclear Research, H-4001 Debrecen, P O Box 51, Hungary
[34]Ludwigs-Maximilians-Universität München, Sektion Physik, Am Coulombwall 1, D-85748 Garching, Germany

[a] and at TRIUMF, Vancouver, Canada V6T 2A3
[b] and Royal Society University Research Fellow
[c] and Institute of Nuclear Research, Debrecen, Hungary
[d] and Department of Experimental Physics, Lajos Kossuth University, Debrecen, Hungary
[e] and Department of Physics, New York University, NY 1003, USA

1 Introduction

The lifetimes of b flavoured hadrons are related both to the strengths of the b quark couplings to c and u quarks, described by the CKM matrix elements $V_{\rm cb}$ and $V_{\rm ub}$, respectively, and to the dynamics of b hadron decays. The spectator model assumes that the light quarks in b and c hadrons do not affect the decay of the heavy quark, and thus predicts the lifetimes of all b hadrons to be equal. For charm hadrons this prediction is inaccurate; non-spectator effects, such as interference between different decay modes, result in a D^+ lifetime approximately 2.5 times that of the D^0 and more than twice that of the D_s^- [1]. Models which attempt to account for non-spectator effects predict that the differences among b hadron lifetimes are much smaller than those in the charm system due to the larger mass of the b quark [2, 3, 4]. These models predict a difference in lifetime between the B^+ and B^0 meson of several percent, and between the B_s^0 and B^0 meson of about 1% [3, 4]. OPAL [5, 6], and other collaborations [7], have published measurements of the B_s^0 lifetime which are in agreement with these models.

Non-spectator decays of B mesons proceeding via W-exchange are Cabibbo-allowed but are expected to be suppressed, relative to spectator decays, by an amount depending on the ratio of the initial-state meson mass and the final-state quark masses (helicity-suppression). This suppression does not occur for baryon decay, therefore b baryon lifetimes are expected to be shorter than b meson lifetimes. This expectation is consistent with existing lifetime measurements [1] for which $\tau(\Lambda_\mathrm{b}^0)/\tau(\mathrm{B}^0) = 0.73 \pm 0.06$ [1]. It is also supported by a recent theoretical prediction [3] which yields $\tau(\Lambda_\mathrm{b}^0)/\tau(\mathrm{B}^0)$ of about 0.9. Reference [4] finds this ratio to be $0.98 + \mathcal{O}(1/m_\mathrm{b}^3)$. Measurements of the average b baryon lifetime have been published based both on analyses of $\Lambda\ell^-$ and $\Lambda_\mathrm{c}^+\ell^-$ correlations by OPAL [8, 9] and other collaborations [10]. In both analyses, the dominant contribution is expected to come from Λ_b^0 baryons, though both $\Lambda\ell^-$ and $\Lambda_\mathrm{c}^+\ell^-$ combinations can arise from the decays of other b baryons. The composition of each sample depends on the b baryon production fractions, but the $\Lambda_\mathrm{c}^+\ell^-$ correlations provide a purer sample of Λ_b^0 baryons.

This paper presents updated measurements of the B_s^0 meson and Λ_b^0 baryon lifetimes using $\mathrm{D}_\mathrm{s}^-\ell^+$ and $\Lambda_\mathrm{c}^+\ell^-$ combinations reconstructed from the full OPAL hadronic data sample collected on or near the Z^0 resonance. These results supersede the previous OPAL measurements using $\mathrm{D}_\mathrm{s}^-\ell^+$ [5] and $\Lambda_\mathrm{c}^+\ell^-$ [8] combinations. The decay channels used for these lifetime measurements are:[1]

$$
\begin{array}{lll}
\mathrm{B}_\mathrm{s}^0 \to \mathrm{D}_\mathrm{s}^-\,\ell^+\,\nu\,\mathrm{X} & & \Lambda_\mathrm{b}^0 \to \Lambda_\mathrm{c}^+\,\ell^-\,\bar{\nu}\,\mathrm{X} \\
\quad \hookrightarrow\ \mathrm{K}^{*0}\,\mathrm{K}^-, & \mathrm{K}^{*0} \to \mathrm{K}^+\pi^- & \quad \hookrightarrow\ \mathrm{pK}^-\pi^+ \\
\quad \hookrightarrow\ \phi\,\pi^-, & \phi \to \mathrm{K}^+\mathrm{K}^- & \quad \hookrightarrow\ \Lambda\ell^+\nu\mathrm{X}, \qquad \Lambda \to \mathrm{p}\pi^- \\
\quad \hookrightarrow\ \mathrm{K}_\mathrm{S}^0\,\mathrm{K}^-, & \mathrm{K}_\mathrm{S}^0 \to \pi^+\pi^- & \\
\quad \hookrightarrow\ \phi\ell^-\bar{\nu}\mathrm{X}, & \phi \to \mathrm{K}^+\mathrm{K}^- &
\end{array}
$$

where ℓ is an electron or a muon. In each case, the proper decay time of the b hadron is determined on an event-by-event basis using measured decay lengths and estimates of the b hadron energy.

The following section provides a brief description of the OPAL detector. The remaining sections describe the selection of $\mathrm{D}_\mathrm{s}^-\ell^+$ and $\Lambda_\mathrm{c}^+\ell^-$ candidates, the determination of the b hadron decay lengths, the estimation of the b hadron boost, the lifetime fits, the results, and the systematic errors.

[1] In this paper, charge conjugate modes are always implied.

2 The OPAL Detector

The OPAL detector is described in detail in reference [11]. The central tracking system is composed of a precision vertex drift chamber, a large volume jet chamber surrounded by a set of chambers which measure the z-coordinate[2] and, for the majority of the data used in this analysis, a high-precision silicon microvertex detector. These detectors are located inside a solenoidal coil. The detectors outside the solenoid consist of a time-of-flight scintillator array and a lead glass electromagnetic calorimeter with a presampler, followed by a hadron calorimeter consisting of the instrumented return yoke of the magnet, and several layers of muon chambers. Charged particles are identified by their specific energy loss per unit length, $\mathrm{d}E/\mathrm{d}x$, in the jet chamber. Further information on the performance of the tracking and $\mathrm{d}E/\mathrm{d}x$ measurements can be found in reference [12].

3 Monte Carlo Simulation

Monte Carlo simulation samples of inclusive hadronic Z^0 decays and of the specific decay modes of interest are used to check the selection procedure and lifetime fit procedure. These samples were produced using the JETSET 7.4 parton shower Monte Carlo generator [13] with the fragmentation function of Peterson et al. [14] for heavy quarks, and then passed through the full OPAL detector simulation package [15]. A special sample of simulated data was generated using a modified JETSET decay routine for b baryons [16], where it is assumed that the polarization of the b quark is carried by the b baryon. An additional form factor [17] describing the energy transfer from the b to c flavoured baryon was used in the generation of the polarized sample.

4 Candidate Selection

This analysis uses data collected during the 1990–1995 LEP running periods at centre-of-mass energies within $\pm 3\,\mathrm{GeV}$ of the Z^0 resonance. After the standard hadronic event selection [18] and detector performance requirements, a sample of 4.4 million events is selected. Jets are defined using charged tracks and electromagnetic clusters not associated with a charged track. These are combined into jets using the scaled invariant mass algorithm with the E0 recombination scheme [19] using $y_{\mathrm{cut}} = 0.04$.

Only charged tracks that are well-measured in the x-y plane are considered in this analysis. Well measured tracks are defined according to standard track quality cuts [20]. Within a single jet, not all combinations of accepted tracks with the appropriate charge combination are considered in the $\mathrm{D}_{\mathrm{s}}^-$ and Λ_{c}^+ searches. Instead, to reduce the combinatorial background, the $\mathrm{d}E/\mathrm{d}x$ probability, w_i, that the observed $\mathrm{d}E/\mathrm{d}x$ is consistent with the assumed particle hypothesis, i, is required to be greater than 1%. More restrictive requirements are imposed on a channel-by-channel basis, as described in the following subsections.

Leptons are identified as follows. Electron candidates with a momentum of at least $2\,\mathrm{GeV}/c$ are identified using an artificial neural network based on twelve measured quantities from the elec-

[2]The right-handed coordinate system is defined such that the z-axis follows the electron beam direction and the x-y plane is perpendicular to it with the x-axis lying approximately horizontally. The polar angle θ is defined relative to the $+z$-axis, and the azimuthal angle ϕ is defined relative to the $+x$-axis.

tromagnetic calorimeter and the central tracking detector [21]. Between 1 and 2 GeV/c, electron candidates are required to have a dE/dx probability of larger than 1% for the electron hypothesis and less than 1% for the proton hypothesis, because it is in this region that the electron and proton dE/dx bands cross. Electron candidates identified as arising from photon conversions are rejected [22]. Muons are identified by associating central detector tracks with track segments in the muon detectors and requiring a position match in two orthogonal coordinates [22].

4.1 Selection of $\mathrm{D_s^-}$ candidates

The $\mathrm{D_s^-}$ candidates are reconstructed in four modes:

1. $\mathrm{D_s^-} \to \mathrm{K^{*0}K^-}$ in which the $\mathrm{K^{*0}}$ decays into a $\mathrm{K^+\pi^-}$.
2. $\mathrm{D_s^-} \to \phi\pi^-$ where the ϕ subsequently decays into $\mathrm{K^+K^-}$.
3. $\mathrm{D_s^-} \to \mathrm{K^-K_S^0}$ where the $\mathrm{K_S^0}$ decays into $\pi^+\pi^-$.
4. The $\mathrm{D_s^-}$ is partially reconstructed in $\mathrm{D_s^-} \to \phi\ell^-\bar{\nu}\mathrm{X}$ where the ϕ decays into $\mathrm{K^+K^-}$.

In all modes except $\phi\ell^-\bar{\nu}\mathrm{X}$, charged kaon candidates are required to have a momentum greater than $2\,\mathrm{GeV}/c$. Also, because of the potential for misidentifying a pion as a kaon, if the observed energy loss of a kaon candidate is greater than the mean expected for a kaon, it must satisfy $w_\mathrm{K} > 5\%$.

In both the $\mathrm{D_s^-} \to \mathrm{K^{*0}K^-}$ and the $\mathrm{D_s^-} \to \phi\pi^-$ channels, if the observed energy losses of both kaon candidates are greater than the mean expected for a kaon, the product of the two dE/dx probabilities must satisfy $w_{\mathrm{K1}} \cdot w_{\mathrm{K2}} > 0.02$. The momentum of the $\mathrm{K^+K^-\pi^-}$ combination is required to be greater than $9\,\mathrm{GeV}/c$ for both channels.

For the $\mathrm{K^{*0}K^-}$ mode, the invariant mass of the $\mathrm{K^+\pi^-}$ combination is required to satisfy $0.845 < m_{\mathrm{K}\pi} < 0.945\,\mathrm{GeV}/c^2$. To reduce the possibility of mistaking a $\mathrm{D^- \to K^{*0}\pi^-}$ decay for the desired signal, the measured dE/dx of the $\mathrm{K^-}$ candidate must be at least one standard deviation below the mean dE/dx that is expected for a pion.

In the $\phi\pi^-$ mode, the observed ϕ width is dominated by detector resolution and the $\mathrm{K^+K^-}$ mass is required to satisfy $1.005 < m_{\mathrm{KK}} < 1.035\,\mathrm{GeV}/c^2$. The momentum of the ϕ candidate is required to be greater than 4.0 GeV/c.

Differences between the angular distributions of $\mathrm{D_s^-}$ decays and those of random track combinations are used to suppress further the combinatorial background. The $\mathrm{D_s^-}$ is a spin-0 meson and the final states of both decay modes consist of a spin-1 (ϕ or $\mathrm{K^{*0}}$) meson and a spin-0 (π^- or $\mathrm{K^-}$) meson. The $\mathrm{D_s^-}$ signal is expected to be uniform in $\cos\theta_p$, where θ_p is the angle in the rest frame of the $\mathrm{D_s^-}$ between the spin-0 meson direction and the $\mathrm{D_s^-}$ direction in the laboratory frame. However, the $\cos\theta_p$ distribution of random combinations peaks in the forward and backward directions. It is therefore required that $|\cos\theta_p| < 0.8$ (0.9) for the $\mathrm{K^{*0}K^-}$ ($\phi\pi^-$) mode. The distribution of $\cos\theta_v$, where θ_v is the angle in the rest frame of the spin-1 meson between the direction of the final state kaon from the decay of the spin-1 meson and the $\mathrm{D_s^-}$ direction, is proportional to $\cos^2\theta_v$ for $\mathrm{D_s^-}$ decays. The $\cos\theta_v$ distribution of the random $\mathrm{K^+K^-\pi^-}$ combinations in the data is, however, approximately flat. Therefore it is required that $|\cos\theta_v| > 0.4$.

For reconstruction of the $\mathrm{D_s^-} \to \mathrm{K^-K_S^0}$ channel, accepted charged kaons are combined with $\mathrm{K_S^0}$ mesons reconstructed in their decays to $\pi^+\pi^-$ as described in [23]. The $\pi^+\pi^-$ mass is required to

satisfy $0.475 < m_{\pi\pi} < 0.525\,\mathrm{GeV}/c^2$. The background of K^0_S particles from fragmentation is reduced by requiring the K^0_S momentum to be greater than $3\,\mathrm{GeV}/c$. To reject background from Λ decays where the proton is misidentified as a pion, K^0_S candidates are rejected if $1.10 < m_{\mathrm{p}\pi} < 1.13\,\mathrm{GeV}/c^2$, where $m_{\mathrm{p}\pi}$ is the invariant mass of the two tracks when the highest momentum track is assigned the proton mass. To improve further the mass resolution of the D_s^-, a fit using kinematic and geometrical constraints is performed. The mass of the two tracks forming the K^0_S is constrained to the known K^0_S mass [1]. Further constraints are applied to the D_s^- and K^0_S, in which the directions of the vectors between their production and decay points are constrained to be the same as the reconstructed momentum vectors.

For the $\mathrm{D}_\mathrm{s}^- \to \phi\ell^-\bar{\nu}\mathrm{X}$ selection, the purity of the kaons from the ϕ decay is enhanced by applying additional pion rejection. This requires that the $\mathrm{d}E/\mathrm{d}x$ probability for the pion hypothesis be less than 40% for tracks whose momenta are such that the mean $\mathrm{d}E/\mathrm{d}x$ for pions is higher than that of kaons, and less than 1% for low momentum tracks where the mean $\mathrm{d}E/\mathrm{d}x$ for kaons is higher than that of pions. Additionally, the product of the $\mathrm{d}E/\mathrm{d}x$ probabilities for a pion hypothesis for the two kaon candidates must be less than 0.018. The ϕ candidate momentum is required to be greater than $4.6\,\mathrm{GeV}/c$. The lepton candidate is required to have a momentum greater than $1\,\mathrm{GeV}/c$ for electrons and $2\,\mathrm{GeV}/c$ for muons. The invariant mass of the $\phi\ell^-$ combination must be less than $1.9\,\mathrm{GeV}/c^2$.

4.2 Selection of Λ_c^+ candidates

The Λ_c^+ candidates are reconstructed in two modes; $\Lambda_\mathrm{c}^+ \to \mathrm{pK}^-\pi^+$ and $\Lambda_\mathrm{c}^+ \to \Lambda\ell^+\nu\mathrm{X}$. In the $\mathrm{pK}^-\pi^+$ selection, the proton, kaon and pion momenta are required to be greater than 3, 2 and 1 GeV/c, respectively. If the observed energy loss of the proton or kaon candidate is greater than the mean $\mathrm{d}E/\mathrm{d}x$ expected for that particle, the corresponding $\mathrm{d}E/\mathrm{d}x$ probability is required to be greater than 3%. The $\mathrm{d}E/\mathrm{d}x$ probability of the pion hypothesis for the proton candidate is required to be less than 1%, which substantially reduces the combinatorial background. The $\mathrm{pK}^-\pi^+$ combination must have a momentum greater than $9\,\mathrm{GeV}/c$. To reduce the possibility of mistaking the decay $\mathrm{D}_\mathrm{s}^+ \to \phi(\mathrm{K}^+\mathrm{K}^-)\pi^+$ for a Λ_c^+ decay by misidentifying the K^+ as a proton, candidates are rejected if the invariant mass of the pK^- combination, when the proton candidate is assigned the kaon mass, is within $10\,\mathrm{MeV}/c^2$ of the nominal ϕ mass [1].

In the $\Lambda_\mathrm{c}^+ \to \Lambda\ell^+\nu\mathrm{X}$ selection, Λ candidates are identified via the decay $\Lambda \to \mathrm{p}\pi^-$. The selection procedure is similar to the one used in reference [9]. The track with the larger momentum is assumed to be the proton and its momentum is required to be larger than 3.0 GeV/c. The other track is required to have a momentum larger than $0.8\,\mathrm{GeV}/c$. The selection criteria for the lepton are the same as described in the previous section for the selection of D_s^- semileptonic decays. The invariant mass of the $\Lambda\ell^+$ combination is required to be less than $2.2\,\mathrm{GeV}/c^2$.

4.3 $\mathrm{D}_\mathrm{s}^-\ell^+$ and $\Lambda_\mathrm{c}^+\ell^-$ selection and decay length determination

Once a combination of tracks that satisfies the D_s^- or Λ_c^+ candidate selection is found, a search is performed to find a lepton from b hadron decay of opposite charge in the same jet. Lepton candidates are identified as described in the introduction to section 4. Both the electron and muon candidates are required to have a momentum greater than $2\,\mathrm{GeV}/c$ except in the $\mathrm{D}_\mathrm{s}^- \to \mathrm{K}^-\mathrm{K}^0_\mathrm{S}$ mode where a higher momentum cut of $5\,\mathrm{GeV}/c$ is used to improve the signal to background

ratio. It is also required that the lepton candidate track be measured precisely by either the silicon microvertex detector or the vertex drift chamber.

To further suppress combinatorial background, requirements are made on the invariant mass and momentum of the $D_s^- \ell^+$ and $\Lambda_c^+ \ell^-$ candidate combinations. $K^+K^-\pi^-\ell^+$ combinations are required to have a mass between 3.2 and 5.5 GeV/c^2 and momentum larger than 17 GeV/c. $K^-K_S^0\ell^+$ combinations are accepted if they have an invariant mass between 3.4 and 5.5 GeV/c^2 and a momentum greater than 17 GeV/c. The $\phi\ell^-\ell^+$ mass is required to be less than 4.8 GeV/c^2 and its momentum greater than 12 GeV/c. Also, for the $\phi\ell^-\ell^+$ mode, the invariant mass of the ϕ and the ℓ^+ must be greater than 2.1 GeV/c^2. In conjunction with the invariant mass cut on the $\phi\ell^-$ pair, this unambiguously separates the leptons from the B_s^0 and D_s^- decays. The $pK^-\pi^+\ell^-$ combination must have a mass between 3.5 and 5.5 GeV/c^2 and momentum greater than 17 GeV/c. In the $\Lambda\ell^+\ell^-$ channel, combinations are accepted if the $\Lambda\ell^+\ell^-$ invariant mass is greater than 2.5 GeV/c^2 and less than 5 GeV/c^2 and the invariant mass of the Λ and ℓ^- is greater than 2.2 GeV/c^2. Furthermore, the cosine of the opening angle between the lepton and the D_s^- or Λ_c^+ candidate must be greater than 0.4.

Three vertices — the beam spot, the B_s^0 (Λ_b^0) decay vertex and the D_s^- (Λ_c^+) decay vertex — are reconstructed in the x-y plane. The beam spot is measured using charged tracks with a technique that follows any significant shifts in the beam spot position during a LEP fill [24]. The intrinsic width of the beam spot in the y direction is taken to be 8 μm. The width in the x direction is measured directly and found to vary between 100 μm and 160 μm.

The D_s^- (Λ_c^+) vertex is fitted in the r-ϕ plane using all the candidate tracks. The B_s^0 (Λ_b^0) decay vertex is formed by extrapolating the candidate D_s^- (Λ_c^+) momentum vector from its decay vertex to the intersection with the lepton track. The D_s^- (Λ_c^+) decay length is the distance between these two decay vertices. The B_s^0 (Λ_b^0) decay length is found by a fit between the beam spot and the reconstructed B_s^0 (Λ_b^0) decay vertex using the direction of the candidate $D_s^-\ell^+$ ($\Lambda_c^+\ell^-$) momentum vector as a constraint. The two-dimensional projections of the B_s^0 (Λ_b^0) and D_s^- (Λ_c^+) decay lengths are converted into three dimensions using the polar angles that are reconstructed from the momenta of the $D_s^-\ell^+$ ($\Lambda_c^+\ell^-$) and D_s^- (Λ_c^+). Typical decay lengths for the $D_s^-\ell^+$ ($\Lambda_c^+\ell^-$) vertex are about 0.3 cm and the corresponding decay length errors range from about 0.03 cm for the $K^+K^-\pi^-$, $\phi\ell^-\bar{\nu}$ and $pK^-\pi^+$ modes, to about twice this level for the modes which include a Λ or K_S^0.

Additional criteria are used to select $D_s^-\ell^+$ and $\Lambda_c^+\ell^-$ candidates suitable for precise decay length measurements. In channels in which a charm state is fully reconstructed the χ^2 of the charm vertex fit is required to be less than 10 (for 1 degree of freedom). Finally, the decay length error of the reconstructed B_s^0 (Λ_b^0) candidate must be less than 0.2 cm.

4.4 Results of $D_s^-\ell^+$ and $\Lambda_c^+\ell^-$ selections

The invariant mass distributions obtained in each of the D_s^- decay modes are shown in figure 1. The equivalent distributions for the reconstructed Λ_c^+ decay modes are shown in figure 2. In each case, the fit result overlaid on the histogram is obtained from an unbinned maximum likelihood fit to the invariant mass distribution. The results of these fits are summarised in table 1.

Each mass fit uses a Gaussian function to describe the signals and a linear parametrization of the combinatorial background. In the $K^+K^-\pi^-$ distributions, a second Gaussian is used to parametrize contributions from the Cabibbo suppressed decay $D^- \to K^+K^-\pi^-$. The mean of this Gaussian is fixed to the nominal D^- mass, 1869.3 MeV/c^2 [1], and the width is constrained to be the same as

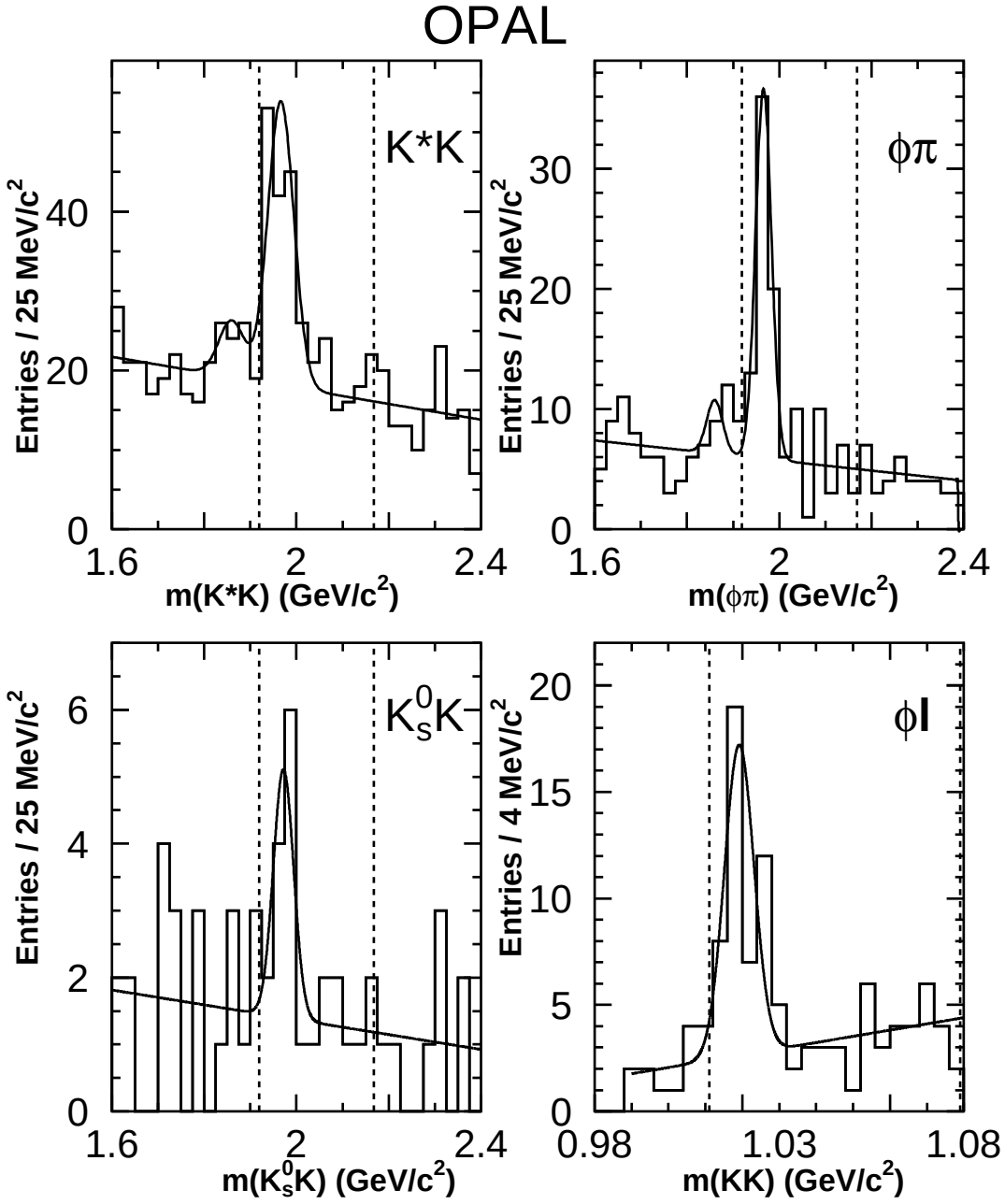

Figure 1: Invariant mass distributions from the four $D_s^- \ell^+$ reconstruction channels. In each plot, the result of the fit described in the text is overlaid as a solid line. The mass ranges used in the decay length fit are shown by the vertical dotted lines.

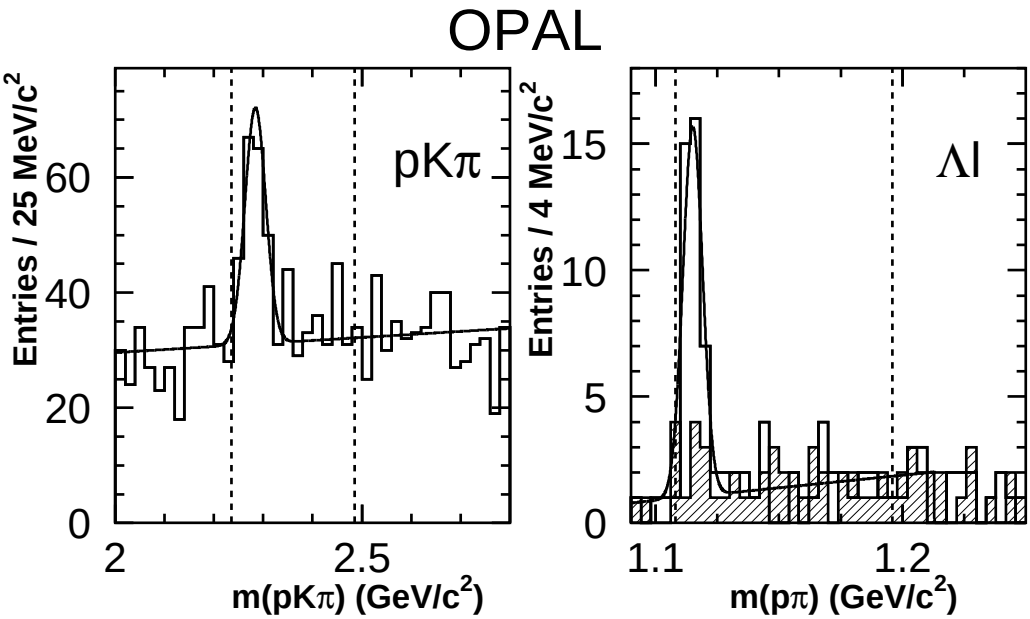

Figure 2: Invariant mass distributions from the two $\Lambda_c^+\ell^-$ reconstruction channels. In each plot, the result of the fit described in the text is overlaid as a solid line. Also indicated are the mass ranges used in the decay length fit. The hatched histogram for the $[\Lambda\ell^+]\ell^-$ channel represents the wrong-sign-Λ combinations: $[\overline{\Lambda}\ell^+]\ell^-$.

that of the D_s^- peak. By integrating the tail of the peak due to the $D^- \to K^+K^-\pi^-$ decays in this D_s^- signal region, the contamination from this source is found to be negligible. No significant peaks are observed in the mass distributions for wrong-sign $D_s^-\ell^-$ ($\Lambda_c^+\ell^+$) combinations in the fully reconstructed decay channels $K^{*0}K^-$, $\phi\pi^-$, $K^-K_S^0$ and $pK^-\pi^+$. The $[\Lambda\ell^+]\ell^-$ combinations[3] include a contribution from Λ baryons from fragmentation that can be estimated from the wrong-sign-Λ distribution, $[\overline{\Lambda}\ell^+]\ell^-$. Studies using simulated data show that the wrong-sign-Λ distribution provides a good representation of these Λ baryons from fragmentation. The $[\overline{\Lambda}\ell^+]\ell^-$ candidates are shown in the plot as a shaded histogram.

For each channel, the fitted mass is consistent with the nominal D_s^- (Λ_c^+) mass [1] and the fitted width is consistent with the expected detector resolution. In total, 199 ± 26 $D_s^-\ell^+$ candidates and 145 ± 24 $\Lambda_c^+\ell^-$ candidates are observed. The $D_s^-\ell^+$ ($\Lambda_c^+\ell^-$) combinations used in the B_s^0 (Λ_b^0) lifetime fits are selected from regions around the identified invariant mass peaks, including a sufficient number of candidates away from the mass peaks to allow an estimate of the lifetime characteristics of the combinatorial background. There are 509 for the B_s^0 lifetime fit and 632 for the Λ_b^0 lifetime fit.

[3]The bracketed particles are those that are assigned to be the decay products of a Λ_c^+. The invariant mass requirements on $\Lambda\ell$ combinations described in sections 4.2 and 4.3, result in a unique assignment of the two leptons.

Decay channel	Signal candidates	Comb. fraction	Width (MeV)	Fit Range (MeV)	Cands. for fit
K^*K	101±21	0.46±0.06	28±5	−50 - 200	280
$\phi\pi$	53±11	0.24±0.05	17±4	−50 - 200	114
$K^-K^0_S$	8±5	0.39±0.19	22±14	−50 - 200	21
$\phi\ell$	37±10	0.23±0.07	4 (fixed)	−8 - 60	94
$D_s^-\ell^+$ total	199 ± 26				509
$pK\pi$	108±22	0.56±0.06	21±5	−50 - 200	522
$\Lambda\ell$	37±9	0.11±0.05	3.4 ± 0.5	−8 - 80	69(41)
$\Lambda_c^+\ell^-$ total	145 ± 24				632

Table 1: Results of the mass fits to all the signal channels. The second column shows the number of candidates in the signal peak. The estimated fraction of combinatorial background is given in the third. The fourth column gives the signal peak width found by the fit or the constraint that was used in the fit to the invariant mass distribution. The mass range used in the lifetime fit is given in the fifth column and the last column gives the number of candidates in this mass range. For the $[\Lambda\ell^+]\ell^-$ channel the number of wrong-sign-Λ candidates, $[\overline{\Lambda}\ell^+]\ell^-$, is included in brackets.

4.5 Backgrounds to the $B_s^0 \to D_s^-\ell^+$ and $\Lambda_b^0 \to \Lambda_c^+\ell^-$ signal

Potential sources of backgrounds to the B_s^0 (Λ_b^0) signal considered here include decays of other b hadrons that can yield a $D_s^-\ell^+$ ($\Lambda_c^+\ell^-$) final state or other final states that are misidentified as a D_s^- (Λ_c^+) hadron. Other sources are D_s^- (Λ_c^+) hadrons combined with a hadron that has been misidentified as a lepton, and random associations of D_s^- (Λ_c^+) hadrons with genuine leptons. Finally, there is purely combinatorial background. The various physics backgrounds, and the calculation of their contributions relative to that of the signal, are discussed below.

4.5.1 Physics backgrounds to $B_s^0 \to D_s^-\ell^+$

The signal event samples include properly reconstructed $D_s^-\ell^+$ combinations that do not arise from B_s^0 decay. Two decay modes of B^0 and B^+ mesons are considered:

(a) $\overline{B} \to D_s^- DX$, $D \to \ell^+\nu X$ (where D is any non-strange charm meson), and

(b) $B \to D_s^- K\ell^+\nu X$, where K is any type of kaon.

For the signal production and decay sequence, the production rate times branching fraction $f(\overline{b} \to B_s^0) \cdot \mathrm{Br}(B_s^0 \to D_s^-\ell^+\nu X) = 0.85 \pm 0.23\%$ is used [1]. Monte Carlo simulations are used to determine the selection efficiencies for background modes relative to that of the signal mode.

For the background, the probability for a bottom quark to form either a B^+ or B^0 meson is 0.378 ± 0.022 [1] each. For the $B \to D_s^- K\ell^+\nu X$ mode, the measured branching ratio is less than 0.009 at the 90% confidence level [1]. Half of this limit is used as a central value in estimating the contribution of this channel, and the range from zero to 0.009 is taken as the uncertainty. For the other background mode, it is noted that $\mathrm{Br}(B \to D_s D) = 0.049 \pm 0.011$ [1], which is then corrected

using Monte Carlo simulation to include the additional contribution from $B \to D_s DX$ decays. The possibility that all the $B \to D_s X$ modes include an additional charm meson is considered as a systematic error. The effect on the reconstruction efficiency of $\overline{D}$ mesons arising from orbitally excited D mesons is also taken into account. The total contribution from these two sources of backgrounds is estimated to be $11 \pm 4\%$.

4.5.2 Physics backgrounds to $\Lambda_b^0 \to \Lambda_c^+ \ell^-$

The events in the Λ_c^+ peak may include $\Lambda_c^+ \ell^-$ combinations that do not arise from Λ_b^0 decay. The decay modes considered are $B_{u,d} \to \Lambda_c^+ \overline{\Xi}_c X$, $\overline{\Xi}_c \to X \ell^- \bar{\nu}$ and $\overline{B}_{u,d,s} \to \Lambda_c^+ X \ell^- \bar{\nu}$. An estimate of the Λ_b^0 signal contamination from other b baryons is also given.

As before, the reconstruction efficiencies for these background modes are calculated relative to the signal mode from simulated event samples. For the production rate times branching fraction of the signal modes, $f(\overline{b} \to \Lambda_b^0) \cdot \mathrm{Br}(\Lambda_b^0 \to \Lambda_c^+ \ell^- \bar{\nu} X) = 1.35 \pm 0.26\%$ [1] is used.

To estimate the background from the internal-W decay $B \to \Lambda_c^+ \overline{\Xi}_c X$, $\overline{\Xi}_c \to X \ell^- \bar{\nu}$, the measured inclusive branching ratio $\mathrm{Br}(B \to \text{charmed-baryon X}) = 6.4 \pm 1.1\%$ [1] is combined with the measurement [25] $\mathrm{Br}(B \to \Lambda_c^+ X)/\mathrm{Br}(B \to \Lambda_c^- X) = 0.19 \pm 0.13 \pm 0.04$, where B refers only to B mesons containing a $\bar{b}$ quark. It is also assumed that when a Λ_c^+ is produced, a $\overline{\Xi}_c$ is always produced. The average semileptonic branching ratio of the charged and neutral Ξ_c (assuming they are produced at equal rates) is estimated to be $25 \pm 10\%$. This was obtained from the semileptonic branching ratio of the Λ_c^+, using the theoretical prediction of [26] and the measured lifetimes of these baryons [1]. After accounting for the relative efficiency, this mode comprises $2.0 \pm 1.5\%$ of the signal.

The contribution from the external-W decay, $\overline{B} \to \Lambda_c^+ X \ell^- \nu$, was estimated using the 90% confidence level limit $\mathrm{Br}(\bar{B}_{u,d} \to p \ell^- \bar{\nu} X) < 0.16\%$ [27]. It is conservatively assumed that this decay always proceeds through a Λ_c^+ and that a Λ_c^+ is equally likely to decay to a proton or a neutron. Thus, $\mathrm{Br}(B \to \Lambda_c^+ \ell^- \bar{\nu} X) < 0.32\%$ at the 90% confidence level. The analogous decays of B_s^0 mesons are also taken into account by assuming that their branching fraction to $\Lambda_c^+ \ell^- \bar{\nu} X$ is the same as for $B_{u,d}$ and using the hadronization fractions from [1]. Accounting for the relative detection efficiency yields an upper limit for this mode corresponding to 5.7% of the signal. Half of this is taken as the central value for this background and the entire range from zero to 5.7% is considered in estimating the systematic error.

Potential contamination of the $\Lambda_c^+ \ell^-$ signal by decays of b baryons other than Λ_b^0 is also investigated. The principle sources of this contamination are from decays of Ξ_b and Σ_b. There is some evidence for the Ξ_b [28], which is expected to decay weakly [29]. Theoretical predictions [29] for the Σ_b mass suggest that it is large enough to allow strong decay to a Λ_b^0. Accepting this, any non-Λ_b^0 in the signal comes from Ξ_b decays.

Semileptonic decays of Ξ_b baryons to excited charm-strange baryons that decay subsequently to Λ_c^+, or non-resonant decays such as $\Xi_b \to \Lambda_c^+ X \ell^- \bar{\nu}$ can contribute to the $\Lambda_c^+ \ell^-$ sample. The level of these decays is estimated using the B meson system as a guide. The branching ratio for non-strange B decays to $X \ell^+ \nu$, where X is not simply a D or D^* meson, is found to be $3.7 \pm 1.3\%$. This value is obtained by subtracting $\mathrm{Br}(B^0 \to D^- \ell^+ \nu)$ and $\mathrm{Br}(B^0 \to D^{*-} \ell^+ \nu)$ from $\mathrm{Br}(B^0 \to X \ell^+ \nu)$ using the values from reference [1]. The same rate is assumed for the analogous Ξ_b decays mentioned above and the conservative assumption is made that in these decays a Λ_c^+ is always produced. It is further assumed that 20% of the weakly decaying b baryons are Ξ_b, based on the relative

rates of production of the corresponding light-flavoured baryons in Z^0 decays [1]. Using the above branching ratio estimates and reconstruction efficiencies for the signal mode and the modes under consideration here, the contribution to the $\Lambda_c^+\ell^-$ signal from the decays of the Ξ_b is estimated to be about 1% and is, therefore, neglected.

The $\Lambda\ell^+\ell^-$ sample can have additional contributions from the decay of $\Xi_b \to \Xi_c\ell^-\bar{\nu}X$ followed by $\Xi_c \to \Xi\ell^+\nu X$ with $\Xi \to \Lambda\pi$. Assumptions about $\mathrm{Br}(\Lambda_c^+ \to \Lambda X\ell^+\nu)/\mathrm{Br}(\Xi_c \to \Xi X\ell^+\nu)$ and $\mathrm{Br}(\Xi_c \to \Xi X)/\mathrm{Br}(\Lambda_c^+ \to \Lambda X)$ are required to estimate this background if measurements of $\Lambda\ell$ [9, 10] and $\Xi\ell$ [28] production are to be used. In the case of the former ratio, this cannot be trivially related to the ratio of lifetimes because of Pauli Interference effects between the two strange quarks that result from the decay of a Ξ_c, but which are not present in the analogous Λ_c^+ decay [26]. The latter ratio is even harder to predict theoretically, even to the extent of whether one would expect it to be greater than or less than unity [30]. In estimating the systematic error due to this source, the fraction of $\Lambda\ell^+\ell^-$ candidates due to Ξ_b decays is varied from 10% to 50%. The Λ_b^0 lifetime will also be quoted with a functional dependence on the level of Ξ_b contamination in the $\Lambda\ell^+\ell^-$ sample, $f_{\Xi_b/\Lambda\ell^+\ell^-}$, using the average Ξ_b lifetime of $1.39^{+0.34}_{-0.28}$ ps as measured from $\Xi\ell$ correlations [28].

4.5.3 Other backgrounds

The D_s^- (Λ_c^+) candidate may be a misidentified charm hadron if one or more tracks are assigned the wrong particle type. This constitutes an additional source of background which is studied using simulated events. For this background, it is found that the invariant mass distribution around the D_s^- (Λ_c^+) mass is similar to that of the combinatorial background. Such events are therefore considered to be included in the combinatorial background fraction.

The level of background from genuine D_s^- (Λ_c^+) particles which are combined with a hadron that is misidentified as a lepton can be estimated by fitting the invariant mass spectrum of wrong-sign combinations in which the charm candidate and the lepton candidate have the same charge. This assumes that random combinations are equally likely to have right and wrong charge correlations. For each channel where the charm hadron is fully reconstructed, the wrong sign signal is consistent with zero. This is in agreement with what has been found in a related analysis that has greater statistical significance [31]. This background source is therefore neglected.

The background from random associations of a D_s^- (Λ_c^+) with genuine leptons is estimated using simulated data. The contribution is less than one event to each of our samples and is neglected.

In the two modes in which the charm hadron is partially reconstructed from a semileptonic decay channel, $D_s^- \to \phi\ell^+\nu X$ and $\Lambda_c^+ \to \Lambda\ell^-\bar{\nu}X$, there are additional backgrounds to consider. These include the accidental combination of a ϕ (Λ), generally produced in fragmentation, with two leptons which arise from a semileptonic bottom hadron decay, followed by a semileptonic charm hadron decay. In the case of the $\Lambda_c^+\ell^-$ channel, this background is estimated using the observed peak in the Λ invariant mass spectrum for the wrong sign combination formed by an ℓ^- from the bottom hadron decay, an ℓ^+ from the charm hadron decay and a $\overline{\Lambda}$ (whereas signal would be a Λ). Fitting the Λ invariant mass distribution for these wrong sign, $[\overline{\Lambda}\ell^+]\ell^-$, candidates, yields a contribution from this source of 9 ± 5 events. The contribution from random associations of a particle that is not from Λ_c^+ decay with a Λ and a lepton from Λ_b^0 decay is found to be negligible. For the analogous D_s^- decay into $\phi\ell^-\overline{\nu}X$, there is no wrong sign distribution available, and hence simulated events are used to estimate this contribution to be 2.5 ± 0.5 candidates. The potential contribution of leptons from J/ψ decays, which are then combined with a ϕ (either from fragmentation or from a b hadron decay) is also estimated using simulated events to be 0.5 ± 0.3 candidates. Finally, the contribution

from hadrons misidentified as leptons is estimated by selecting events in which the two leptons in these modes have the same sign and is found to contribute 2 ± 2 candidates.

The non-combinatorial background sources mentioned above are expected to contribute a total of 27 ± 11 events to the $\mathrm{D_s^-}\ell^+$ signal and 16 ± 7 events to the $\Lambda_\mathrm{c}^+\ell^-$ signal. The background subtracted number of $\mathrm{D_s^-}\ell^+$ signal candidates is therefore

$$N(\mathrm{B_s^0} \to \mathrm{D_s^-}\ell^+\nu\mathrm{X}) \;=\; 172 \pm 28 \;.$$

The background subtracted number of $\Lambda_\mathrm{c}^+\ell^-$ signal candidates is

$$N(\Lambda_\mathrm{b}^0 \to \Lambda_\mathrm{c}^+\ell^-\bar{\nu}\mathrm{X}) \;=\; 129 \pm 25 \;,$$

where no correction has been made for possible Ξ_b contamination.

5 The $\mathrm{B_s^0}$ and Λ_b^0 Lifetime Fit

To extract the $\mathrm{B_s^0}$ (Λ_b^0) lifetimes from the measured decay lengths, an unbinned maximum likelihood fit is performed using a likelihood function that accounts for both the signal and background components of the sample. This fit is largely the same as has been used previously in similar OPAL measurements [5, 8].

5.1 Boost Determination

For the component of the likelihood function describing the $\mathrm{B_s^0}$ (Λ_b^0) signals, the $\mathrm{B_s^0}$ (Λ_b^0) lifetime must be related to the observed decay lengths. Since neither channel is fully reconstructed, because at least the neutrino produced in the b hadron decay is not reconstructed, it is necessary to estimate the b hadron momentum, p_B. The probability distribution of a given candidate having a particular $\mathrm{B_s^0}$ (Λ_b^0) momentum, $\mathcal{B}$, is estimated on an event-by-event basis in one of two ways, depending on the decay channel.

For the semileptonic $\mathrm{D_s^-}$ decay mode and both Λ_c^+ decay modes, the technique employed in reference [8] is used. This relies on information from Monte Carlo simulation to estimate the probability distribution of b hadron energy, given the observed momentum, p_D^i, and invariant mass, m_D^i of all the observed tracks in the candidate (i.e., $\mathrm{K^+K^-}\ell^-\ell^+$, $\mathrm{pK^-}\pi^+\ell^-$ or $\mathrm{p}\pi^-\ell^+\ell^-$). Using a conversion factor, $R \equiv p_\mathrm{D}^i/p_\mathrm{B}$, the relationship of the decay time, t, to the decay length L, can be expressed as $t = L \cdot R \cdot (m_\mathrm{B}/p_\mathrm{D}^i)$, where m_B is the $\mathrm{B_s^0}$ (Λ_b^0) mass. The distribution of R was determined using simulated data for the signal Λ_c^+ decay modes and the semileptonic $\mathrm{D_s^-}$ decay mode produced with the JETSET 7.4 Monte Carlo [13], using the fragmentation function of Peterson et al. [14]. For each decay mode, twelve R distributions were produced covering different ranges of the momentum and invariant mass of the $\mathrm{D_s^-}\ell^+$ ($\Lambda_\mathrm{c}^+\ell^-$) combination. These distributions are used in the lifetime fit to describe the probability, $\mathcal{B}(p_\mathrm{B} \mid p_\mathrm{D}^i, m_\mathrm{D}^i)$ that a candidate with a measured p_D^i and m_D^i will have a particular $\mathrm{B_s^0}$ (Λ_b^0) momentum.

For the other $\mathrm{D_s^-}$ decay modes in which the $\mathrm{D_s^-}$ is fully reconstructed, an analytic approach is used [5, 31]. This approach is not applicable in the case of the Λ_b^0 decays because of the possibility of large polarization effects. The same momentum and invariant mass observables (p_D^i and m_D^i) as the other method are employed, but an exact calculation is used, based on the kinematics of the $\mathrm{B_s^0} \to \mathrm{D_s^-}\ell^+\nu\mathrm{X}$ decay rather than Monte Carlo simulation, to calculate the probability distribution $\mathcal{B}(p_\mathrm{B} \mid p_\mathrm{D}^i, m_\mathrm{D}^i)$. This approach is described in detail in reference [31].

5.2 Likelihood Functional Form

The likelihood function for observing a particular decay length of a $\mathrm{B_s^0}$ (Λ_b^0) hadron may now be parametrized in terms of the measurement error of the decay length, the $\mathrm{D_s^-}\ell^+$ ($\Lambda_\mathrm{c}^+\ell^-$) invariant mass and momentum, and the assumed lifetime. The functional form of the likelihood is given by the convolution of three terms: an exponential whose mean is the $\mathrm{B_s^0}$ (Λ_b^0) lifetime, the boost distribution obtained from the values of the observed $\mathrm{D_s^-}\ell^+$ ($\Lambda_\mathrm{c}^+\ell^-$) mass and momentum, and a Gaussian resolution function with width equal to the measured decay length error. This can be expressed as:

$$\mathcal{L}_i^\mathrm{B}(L^i \mid \tau_\mathrm{B}, \sigma_L^i, p_\mathrm{D}^i, m_\mathrm{D}^i) = \int_0^\infty \mathrm{d}l \int_0^{p_\mathrm{B}^\mathrm{max}} \mathrm{d}p_\mathrm{B} \;\; \mathcal{G}(L^i \mid l, \sigma_L^i) \;\; \mathcal{B}(p_\mathrm{B} \mid p_\mathrm{D}^i, m_\mathrm{D}^i) \;\; \mathcal{P}(l \mid \tau_\mathrm{B}, p_\mathrm{B}) \;, \qquad (1)$$

where $p_\mathrm{B}^\mathrm{max}$ is the maximum possible energy that the b hadron can have. The function $\mathcal{G}$ is a Gaussian function that describes the probability to observe a decay length, L^i, given a true decay length l and the measurement uncertainty σ_L^i. $\mathcal{B}$ is the probability of a particular $\mathrm{B_s^0}$ (Λ_b^0) momentum for an observed momentum, p_D^i and invariant mass, m_D^i of all tracks comprising the candidate. $\mathcal{P}$ is the probability for a given $\mathrm{B_s^0}$ (Λ_b^0) to decay at a distance l from the $\mathrm{e^+e^-}$ interaction point. This function is given by:

$$\mathcal{P}(l \mid \tau_\mathrm{B}, p_\mathrm{B}) = \frac{m_\mathrm{B}}{\tau_\mathrm{B} p_\mathrm{B}} \exp\left[\frac{-l \cdot m_\mathrm{B}}{\tau_\mathrm{B} p_\mathrm{B}}\right] \;, \qquad (2)$$

where $\tau_\mathrm{B} p_\mathrm{B}/m_\mathrm{B}$ is the mean decay length for a given momentum, p_B, mean lifetime, τ_B, and mass, m_B, of the $\mathrm{B_s^0}$ (Λ_b^0).

As discussed previously, non-combinatorial (physics) backgrounds result from the decay of other b hadrons. The likelihood function describing these sources of background is therefore taken to have the same form as the $\mathrm{B_s^0}$ (Λ_b^0) signal, except that the b hadron lifetimes contributing to these background samples are fixed to the exclusive world average values [1], weighted appropriately. The level of the contributions to this background are set to fixed fractions of the signal, as determined in the previous section. The effects of the uncertainty in these fractions on the lifetime are addressed as a systematic error. The likelihood function, $\mathcal{L}_i^{\mathrm{D}\ell(\Lambda\ell)}$, describing all sources of $\mathrm{D_s^-}\ell^+$ ($\Lambda_\mathrm{c}^+\ell^-$) combinations — the $\mathrm{B_s^0}$ (Λ_b^0) signal as well as these physics backgrounds — is just a linear combination of $\mathcal{L}_i^\mathrm{B}$ and the physics background contributions. For the semileptonic channels, the lifetime distribution of the backgrounds which include a real ϕ (Λ) not from a $\mathrm{D_s^-}$ (Λ_c^+), is estimated from the sideband, in the case of $\mathrm{D_s^-}$, or the sideband and the wrong-sign distribution for the Λ_c^+ mode. For the purposes of determining the lifetime properties of the background, these background sources are treated as combinatorial.

The fit must also account for the combinatorial background present in the $\mathrm{D_s^-}\ell^+$ ($\Lambda_\mathrm{c}^+\ell^-$) sample. The functional form used to parametrize this source of background is composed of a positive and a negative exponential, each convolved with the same boost function and Gaussian resolution function as the signal. This can be expressed as,

$$\mathcal{L}_i^\mathrm{comb}(L^i \mid \tau_{bg}^+, \tau_{bg}^-, f_{bg}^+, \sigma_L^i, p_\mathrm{D}^i, m_\mathrm{D}^i) =$$

$$\int_0^\infty \mathrm{d}l \int_0^{p_\mathrm{B}^\mathrm{max}} \mathrm{d}p_\mathrm{B} \;\; \mathcal{G}(L^i \mid l, \sigma_L^i) \;\; \mathcal{B}(p_\mathrm{B} \mid p_\mathrm{D}^i, m_\mathrm{D}^i) \;\; \mathcal{P}_{bg}(L \mid \tau_{bg}^+, \tau_{bg}^-, f_{bg}^+, p_\mathrm{B}) \;, \qquad (3)$$

where

$$\mathcal{P}_{bg}(l \mid \tau_{bg}^+, \tau_{bg}^-, f_{bg}^+, p_\mathrm{B}) = f_{bg}^+ \frac{m_\mathrm{B}}{\tau_{bg}^+ p_\mathrm{B}} \exp\left[\frac{-l \cdot m_\mathrm{B}}{\tau_{bg}^+ p_\mathrm{B}}\right] + (1 - f_{bg}^+) \frac{m_\mathrm{B}}{|\tau_{bg}^-| p_\mathrm{B}} \exp\left[\frac{-(-l) \cdot m_\mathrm{B}}{|\tau_{bg}^-| p_\mathrm{B}}\right] \;. \qquad (4)$$

The fraction of background with positive lifetime, f_{bg}^{+}, as well as the characteristic positive and negative lifetimes of the background, τ_{bg}^{+} and τ_{bg}^{-}, are free parameters in the fit. This double-exponential shape is motivated by considerations of event topologies that can lead to apparent negative decay lengths, even before resolution effects are considered. The background parameters are fitted separately for the hadronic and semileptonic $\mathrm{D_s^-}$ (Λ_c^+) modes, since the lifetime properties of the real ϕ (Λ) backgrounds may well be different from the purely combinatorial background in the other decay modes.

The background in the event sample is taken into account by simultaneously fitting for the signal and background contributions. The probability that a candidate arises from combinatorial background, f_i^{comb}, is determined as a function of the observed invariant mass of this candidate from the fits to the invariant mass spectra shown in figures 1 and 2.

Thus, the full likelihood for candidate i is:

$$\mathcal{L}_i(L^i \mid \tau_\mathrm{B}, \sigma_L^i, p_\mathrm{D}^i, m_\mathrm{D}^i) \;=\; (1 - f_i^{\mathrm{comb}}) \cdot \mathcal{L}_i^{\mathrm{D}\ell(\Lambda\ell)} \;+\; f_i^{\mathrm{comb}} \cdot \mathcal{L}_i^{\mathrm{comb}} \;. \tag{5}$$

In total, four parameters are free in the fit: the $\mathrm{B_s^0}$ (Λ_b^0) lifetime, and the parameters describing the combinatorial background (f_{bg}^{+}, τ_{bg}^{+} and τ_{bg}^{-}).

5.3 Lifetime Fit Results

The fit to the decay lengths of the 509 $\mathrm{D_s^-}\ell^+$ combinations yields $\tau(\mathrm{B_s^0}) = 1.50^{+0.16}_{-0.15}$ ps, where the error is statistical only. The fit to the 632 $\Lambda_\mathrm{c}^+\ell^-$ candidates yields $\tau(\Lambda_\mathrm{b}^0) = 1.26^{+0.23}_{-0.20}$ ps.[4] The results of these fits are shown in figures 3 and 4. In each figure, the candidates are divided into two categories — signal region and sideband region — in order to show the behaviour of the fit when the candidate sample consists mostly of signal or mostly of combinatorial background. The signal region is defined as the mass region within two standard deviations of the fitted invariant mass (see figures 1 and 2). The curves in these figures represent the sums of the decay length probability distributions for each event. The figures indicate that the fitted functional forms provide a good description of the data for both signal and background. For the $\mathrm{B_s^0}$ (Λ_b^0) fit, a total χ^2 of 5.2 (9.6) is found for the sum of the signal and sideband decay length distributions for 12 (11) bins that contain at least five candidates. As was stated earlier, the fits are to unbinned data.

6 Checks of the Method

Tests are performed on several samples of simulated events to check for biases in the selection and fitting procedures. The first tests involve a simple Monte Carlo program which generates decay length data for the signal $\mathrm{D_s^-}\ell^+$ ($\Lambda_\mathrm{c}^+\ell^-$) decays and combinatorial background. For each signal candidate from a $\mathrm{B_s^0}$ (Λ_b^0) decay, this simulation generates a $\mathrm{B_s^0}$ (Λ_b^0) decay time from an exponential distribution with the mean set to a known value. The $\mathrm{B_s^0}$ (Λ_b^0) momenta are chosen from a spectrum based on the full Monte Carlo simulation. The $\mathrm{B_s^0}$ (Λ_b^0) decay length is then calculated and combined with the momentum to give the true candidate decay time. This is then degraded by a resolution function. Physics backgrounds are generated through a similar procedure. Many

[4] In comparing these two measurements, note that the fractional errors do not scale directly with the number of events in the signal because of the larger combinatorial background in the $\mathrm{pK^-\pi^+\ell^-}$ mode, which is the statistically dominant mode for the Λ_b^0 lifetime measurement.

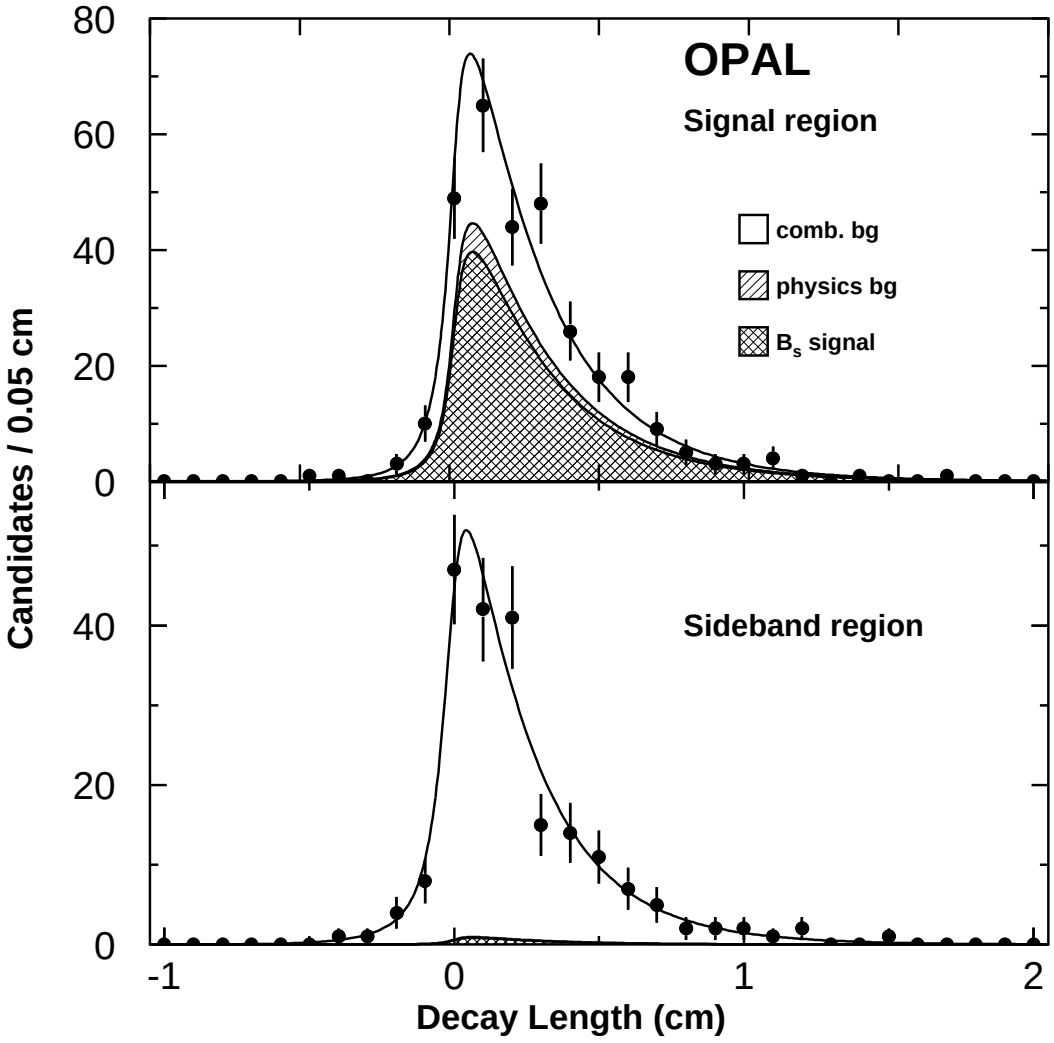

Figure 3: Top: The decay length distribution of $D_s^- \ell^+$ combinations with an invariant mass within the signal region. The unhatched area represents the contribution from combinatorial background, the hatched area is the contribution from sources of non-combinatorial background and the double-hatched region is due to signal from decays of a B_s^0. Bottom: The similar decay length distribution for candidates with an invariant mass in the sideband region. The curves are the results of the fit described in the text.

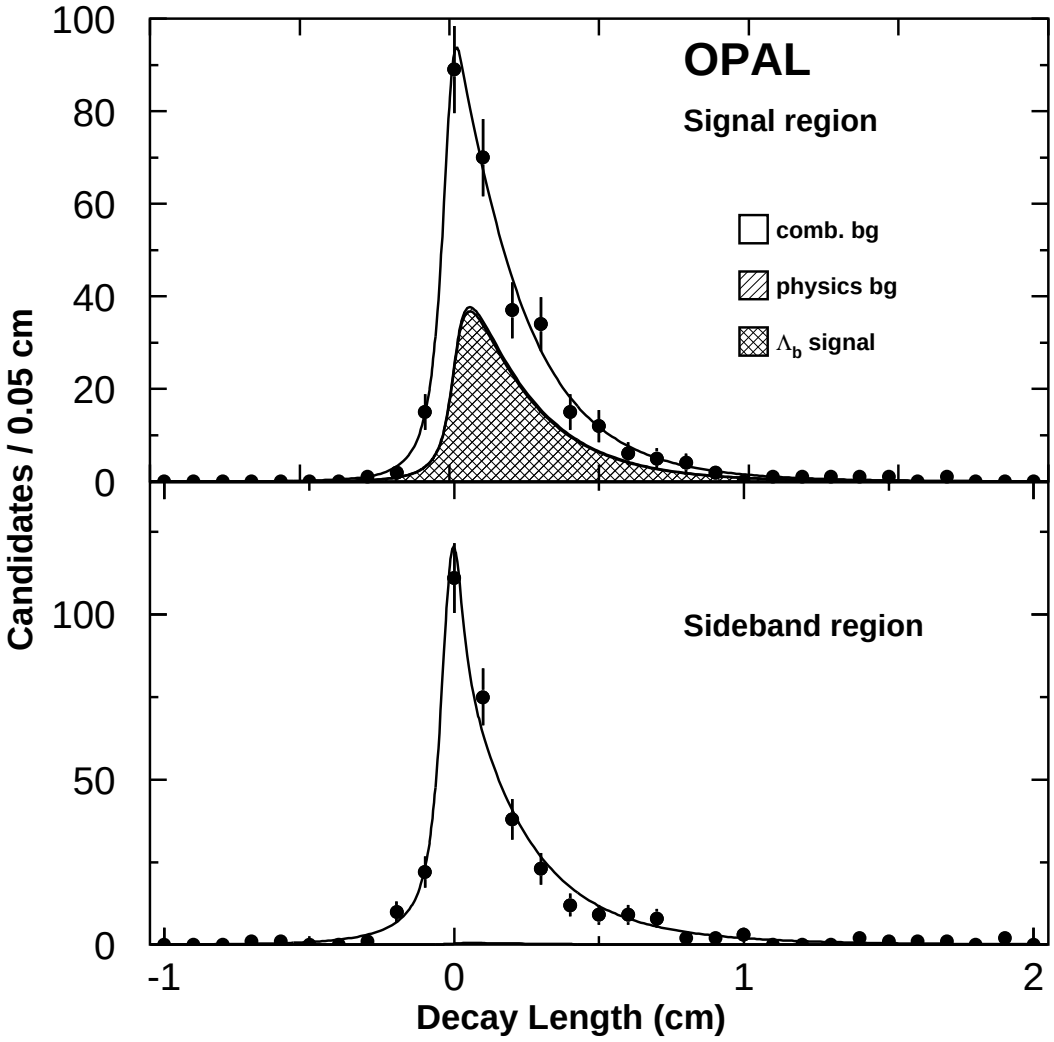

Figure 4: Top: The decay length distribution of $\Lambda_c^+\ell^-$ combinations with an invariant mass within the signal region. The unhatched area represents the contribution from combinatorial background, the (very small) hatched region represents non-combinatorial background, not including any Ξ_b contribution, and the double-hatched area is due to signal from decays of a Λ_b^0. Bottom: The similar decay length distribution for candidates with an invariant mass in the sideband region. The curves are the results of the fit described in the text.

fits are conducted over wide ranges of B_s^0 (Λ_b^0) lifetimes with different levels and parametrizations of the backgrounds. The results of these studies show no biases in the fitted B_s^0 (Λ_b^0) lifetime to a level of less than 0.5% and that the statistical precision of the fit to data is consistent with the sample size and composition.

To verify that the $D_s^- \ell^+$ ($\Lambda_c^+ \ell^-$) selection does not bias the reconstructed sample, lifetime measurements are made using simulated event samples in which large numbers of the decays of interest are produced. In these tests it is found that the mean lifetime of the selected sample of candidates is consistent with the lifetime used to generate the sample, indicating no bias in the selection procedure. Applying the lifetime fit to the selected samples similarly shows no evidence for a bias to within the statistical precision allowed by these samples. This precision ranged from 2% for the $K^+K^-\pi^-$ and $pK^-\pi^+$ channels to 4% for the other decay modes. Similarly, applying the selection and fitting procedure to a Monte Carlo simulation sample of 4 million hadronic Z^0 decays, the fitted B_s^0 (Λ_b^0) lifetimes agree with the generated lifetimes to within the statistical power of the sample.

The lifetime fit is also applied to each decay channel individually. The resulting lifetimes of these separate fits are consistent with each other and with the fit to the entire sample.

7 Evaluation of Systematic Errors

The sources of systematic error considered are those due to the level, parametrization and source of the background, the boost estimation method, possible polarization of b baryons, the beam spot determination and possible tracking errors. These systematic errors are summarized in table 2.

The uncertainty in the level of combinatorial background has two sources: the uncertainty due to the mass fit to the candidate invariant mass spectra and the statistical variation of the background under the invariant mass peak. Background fractions due to one standard deviation variations for these two cases are determined and used in the lifetime fit. This produces variations in the B_s^0 and Λ_b^0 lifetimes of ± 0.03 ps. The width of the sideband region of the mass spectra, from which candidates are selected for use in the lifetime fit, is also varied yielding contributions to the systematic errors of ± 0.01 ps for the B_s^0 and ± 0.03 ps for the Λ_b^0 lifetimes. Using a quadratic function to describe the mass distribution of the combinatorial background has a negligible effect on the fitted lifetimes.

The effect of the uncertainty in the level of the non-combinatorial backgrounds to the B_s^0 and Λ_b^0 signal is estimated by varying these background levels over the ranges described in section 4.5. This produces a ± 0.01 ps variation in the B_s^0 lifetime. The systematic shift due to a Ξ_b contamination of $30 \pm 20\%$ in the Λ_b^0 sample is $+0.02 \pm 0.02$ ps. The shift in the central value of the measured lifetime as a function of Ξ_b contamination is $+0.08 \cdot f_{\Xi_b/\Lambda\ell^+\ell^-}$ ps. All other non-combinatorial backgrounds mentioned in section 4.5 contribute an additional error of ± 0.01 ps to the Λ_b^0 lifetime. The b hadron lifetimes used for these backgrounds are also varied within their measured errors [1]. The resulting change in the fitted lifetimes is less than ± 0.01 ps.

The total systematic error associated with the description of the combinatorial and physics backgrounds is therefore ± 0.03 ps (± 0.05 ps) for the measured B_s^0 (Λ_b^0) lifetimes.

The effects of uncertainty in the b hadron fragmentation are estimated slightly differently for the two boost estimation methods employed. For the hadronic D_s^- decay modes, the estimated B_s^0 energy spectrum used by the boost estimation procedure is varied within the measured limits of the average b hadron energy [32]. Similarly, in generating the Monte Carlo events used to estimate

the b hadron boost for the two Λ_c^+ decay modes and the $\phi\ell^-$ mode, the average b hadron energy was varied by the same amounts as used above. These variations yield changes in the fitted lifetimes of ± 0.02 ps. The effect on the lifetime of varying the mass of the Λ_b^0 by $\pm 50\,\mathrm{MeV}/c^2$ about its central value of $5641\,\mathrm{MeV}/c^2$ [1] is ± 0.01 ps. The effect of a $2\,\mathrm{MeV}/c^2$ uncertainty in the mass of the B_s^0 [1] results in a change of less than 0.01 ps in the measured B_s^0 lifetime.

In the Monte Carlo events used for the boost estimate, the Λ_b^0 was assumed to be unpolarized. However, in the Standard Model, b baryons can retain up to the full longitudinal polarization of -0.94 from the b quark. A variation from 0 to -0.94 polarization produces a change of $+0.06$ ps. A recent measurement of the polarization [33] is used to correct the lifetime extracted using the decay length fit. This yields a correction of $+0.014^{+0.020}_{-0.014}$ ps, where this error results from the precision of the polarization measurement. The effect of the choice of form factor used to describe the energy transfer from the Λ_b^0 to the Λ_c^+ has also been investigated. The use of the alternative form factors of reference [17] produces a negligible change in the fitted lifetime.

The average interaction point of the LEP beams in OPAL is used as the estimate of the production vertex of the B_s^0 and Λ_b^0 candidates. The mean coordinates of the beam spot are known to better than $25\,\mu$m in the x direction and $10\,\mu$m in y. The effective r.m.s. spread of the beam is known to a precision of better than $10\,\mu$m in both directions. To test the sensitivity of $\tau(B_s^0)$ and $\tau(\Lambda_b^0)$ to the assumed position and size of the beam spot, the coordinates of the beam spot are shifted by $\pm 25\,\mu$m, and the spreads are changed by $\pm 10\,\mu$m. The largest observed variation in $\tau(B_s^0)$ and $\tau(\Lambda_b^0)$ is 0.01 ps which is assigned as a systematic error to both measurements.

The effects of alignment and calibration uncertainties on the result are not studied directly but are estimated from a detailed study of 3-prong τ decays [24], in which the uncertainty in the decay length due to these effects is found to be less than 1.8% for the data taken during 1990 and 1991 and less than 0.4% for later data. This corresponds to an uncertainty on $\tau(B_s^0)$ and $\tau(\Lambda_b^0)$ of 0.01 ps. The potential for incorrect estimation of the decay length error is addressed by allowing an additional parameter in the lifetime fit which is a scale factor on the estimated decay length error. This parameter is found to be consistent with unity. This procedure changes the B_s^0 lifetime by less than 0.01 ps and the Λ_b^0 lifetime by -0.02 ps.

Source	$\tau(B_s^0)$ correction (ps)	$\tau(\Lambda_b^0)$ correction (ps)
background (excl. Ξ_b)	0.00 ± 0.03	0.00 ± 0.05
Ξ_b background		$+0.02 \pm 0.02$
uncertainty in boost	0.00 ± 0.02	0.00 ± 0.02
polarization		$+0.01 \pm 0.02$
beam spot	0.00 ± 0.01	0.00 ± 0.01
alignment errors	0.00 ± 0.01	0.00 ± 0.01
total	± 0.04	$+0.03 \pm 0.06$

Table 2: Summary of systematic corrections and uncertainties on the B_s^0 and Λ_b^0 lifetimes.

8 Conclusion

The decay channels $B_s^0 \to D_s^- \ell^+ \nu X$ and $\Lambda_b^0 \to \Lambda_c^+ \ell^- \bar{\nu} X$, where D_s^- decays to $K^{*0}K^-$, $\phi\pi^-$, $K^-K_S^0$ or $\phi\ell^-\bar{\nu}X$ and Λ_c^+ decays to $pK^-\pi^+$ or $\Lambda\ell^+\nu X$ have been reconstructed. From almost 4.4 million hadronic Z^0 events recorded by OPAL from 1990 to 1995, a total of 172 ± 28 such candidates are attributed to B_s^0 decays and 129 ± 25 such candidates are attributed to Λ_b^0 decays.

The B_s^0 lifetime is found to be

$$\tau(B_s^0) = 1.50^{+0.16}_{-0.15} \pm 0.04\,\text{ps},$$

where the first error is statistical and the second systematic. As predicted by theoretical calculations [3, 4], this result is consistent with the observed value for the B^0 lifetime [1]. This is also in agreement with other measurements of the B_s^0 lifetime [6, 7]. The above value of $\tau(B_s^0)$ has been combined with the OPAL measurement of the B_s^0 lifetime in which only a D_s^- candidate is reconstructed [6] which yields $\tau(B_s^0) = 1.72^{+0.20}_{-0.19}(\text{stat})^{+0.18}_{-0.17}(\text{syst})\,\text{ps}$. Taking the correlated statistical and systematic errors into account, the average of these two measurements is found to be $1.57 \pm 0.14\,\text{ps}$.

The measured Λ_b^0 lifetime, is

$$\tau(\Lambda_b^0) = (1.27 + 0.08 \cdot f_{\Xi_b/\Lambda\ell^+\ell^-})^{+0.23}_{-0.20} \pm 0.06\,\text{ps}\ ,$$

where the dependence of the fitted Λ_b^0 lifetime is given in terms of the fraction, $f_{\Xi_b/\Lambda\ell^+\ell^-}$, of the $\Lambda\ell^+\ell^-$ candidates that are due to Ξ_b decays, the first error is statistical and the second systematic. Assuming Ξ_b contamination of $30 \pm 20\%$, the Λ_b^0 lifetime is

$$\tau(\Lambda_b^0) = 1.29^{+0.24}_{-0.22} \pm 0.06\,\text{ps}.$$

The lifetime using the $\Lambda\ell^+\ell^-$ sample alone is found to be $0.85^{+0.53+0.11}_{-0.37-0.14}\,\text{ps}$, when the Ξ_b content is taken to be $30 \pm 20\%$. For the $pK^-\pi^+\ell^-$ sample alone, the Ξ_b content is estimated to be only about 1% and the lifetime of this sample is $1.36^{+0.25}_{-0.23} \pm 0.06\,\text{ps}$. These are consistent with other recent measurements [9, 10] which have tended to be lower than the B^0 meson lifetime in qualitative agreement with the predictions of [3, 4].

Acknowledgements:

We particularly wish to thank the SL Division for the efficient operation of the LEP accelerator at all energies and for their continuing close cooperation with our experimental group. We also thank I.I. Bigi, B. Melic, M. Neubert and M.B. Voloshin for their aid in understanding the present theoretical description of charmed baryon decays. We thank our colleagues from CEA, DAPNIA/SPP, CE-Saclay for their efforts over the years on the time-of-flight and trigger systems which we continue to use. In addition to the support staff at our own institutions we are pleased to acknowledge the
Department of Energy, USA,
National Science Foundation, USA,
Particle Physics and Astronomy Research Council, UK,
Natural Sciences and Engineering Research Council, Canada,
Israel Science Foundation, administered by the Israel Academy of Science and Humanities,
Minerva Gesellschaft,
Benoziyo Center for High Energy Physics,
Japanese Ministry of Education, Science and Culture (the Monbusho) and a grant under the Monbusho International Science Research Program,

German Israeli Bi-national Science Foundation (GIF),
Bundesministerium für Bildung, Wissenschaft, Forschung und Technologie, Germany,
National Research Council of Canada,
Research Corporation, USA,
Hungarian Foundation for Scientific Research, OTKA T-016660, T023793 and OTKA F-023259.

References

[1] Particle Data Group, R.M. Barnett et al., Phys. Rev. **D 54** (1996) 1.

[2] G. Altarelli and S. Petrarca, Phys. Lett. **B 261** (1991) 303;
I. Bigi, Phys. Lett. **B 169** (1986) 101;
J.H. Kühn et al., *Heavy Flavours at LEP*, MPI–PAE/PTh 49/89, August 1989, contribution by R. Rückl, p. 59.

[3] I. Bigi, Nuovo Cim. **109A** (1996) 713;
I. Bigi et al., (CERN-TH.7132/94), from the second edition of the book 'B Decays,' S. Stone (ed.), World Scientific, pp. 132-157;
I.I. Bigi and N.G. Uraltsev, Phys. Lett. **B 280** (1992) 271.

[4] M. Neubert and C.T. Sachrajda, Nucl. Phys. **B 483** (1997) 339.

[5] OPAL Collab., R. Akers et al., Phys. Lett. **B 350** (1995) 273 .

[6] OPAL Collab., K. Ackerstaff et al., "A Measurement of the B_s^0 Lifetime using Reconstructed D_s^- Mesons", CERN-PPE/97-095, submitted to Z. Phys. C.

[7] ALEPH Collab., D. Buskulic et al., Phys. Lett. **B 377** (1996) 205;
ALEPH Collab., D. Buskulic et al., Z. Phys, **C 69** (1996) 585;
CDF Collab., F. Abe et al., Phys. Rev. Lett. **77** (1996) 1945;
CDF Collab., F. Abe et al., Phys. Rev. Lett. **74** (1995) 4988;
DELPHI Collab., P. Abreu et al., Z. Phys. **C 71** (1996) 11.

[8] OPAL Collab., R. Akers et al., Phys Lett. **B 353** (1995) 402.

[9] OPAL Collab., R. Akers et al., Z. Phys. **C 69** (1996) 195.

[10] ALEPH Collab., D. Buskulic et al., "Measurement of the b baryon lifetime and branching fractions in Z decays", CERN-PPE/97-111, submitted to Z. Phys. C;
CDF Collab., F. Abe et al., Phys. Rev. Lett. **77** (1996) 1439;
DELPHI Collab., P. Abreu et al., Z. Phys. **C 71** (1996) 199;
DELPHI Collab., P. Abreu et al., Z. Phys. **C 68** (1995) 375.

[11] OPAL Collab., K. Ahmet et al., Nucl. Inst. and Meth. **A 305** (1991) 275;
P.P. Allport et al., Nucl. Inst. and Meth. **A 324** (1993) 34;
P.P. Allport et al., Nucl. Inst. and Meth. **A 346** (1994) 476.

[12] O. Biebel et al., Nucl. Inst. and Meth. **A 323** (1992) 169;
M. Hauschild et al., Nucl. Inst. and Meth. **A 314** (1992) 74.

[13] T. Sjöstrand, Comp. Phys. Comm. **82** (1994) 74.
The OPAL parameter optimization is described in
OPAL Collab., G. Alexander et al., Z. Phys. **C 69** (1996) 543.

[14] C. Peterson et al., Phys. Rev. **D 27** (1983) 105.

[15] J. Allison et al., Nucl. Inst. and Meth. **A 317** (1992) 47.

[16] A special subroutine for the decays of b-flavoured baryons was provided by T. Sjöstrand.

[17] X.H. Guo and P. Kroll, Z. Phys. **C 59** (1993) 567.

[18] OPAL Collab., G. Alexander et al., Z. Phys. **C 52** (1991) 175.

[19] JADE Collab., W. Bartel et al., Z. Phys. **C 33** (1986) 23;
JADE Collab., S. Bethke et al., Phys. Lett. **B 213** (1988) 235.

[20] OPAL Collab., R. Akers et al., Phys. Lett. **B 316** (1993) 435.

[21] OPAL Collab., R. Akers et al., Phys. Lett. **B 327** (1994) 411.

[22] OPAL Collab., P.D. Acton et al., Z. Phys. **C 58** (1993) 523.

[23] OPAL Collab., R. Akers et al., Z. Phys. **C 67** (1995) 389.

[24] OPAL Collab., P.D. Acton et al., Z. Phys. **C 59** (1993) 183;
OPAL Collab., R. Akers et al., Phys. Lett. **B 338** (1994) 497.

[25] CLEO Collab., R. Ammar et al., Phys. Rev. **D 55** (1997) 13.

[26] B. Guberina and B. Melic, "Inclusive Charmed-Baryon Decays and Lifetimes", IRB-TH 1/97, April 1997;
M.B. Voloshin, Phys. Lett. **B 385** (1996) 369.

[27] ARGUS Collab., H. Albrecht et al., Phys. Lett. **B 249** (1990) 359. The decay used in this reference to measure the branching ratio $\mathrm{Br}(\bar{\mathrm{B}}_{\mathrm{u,d}} \to \mathrm{p}\ell^{-}\bar{\nu}\mathrm{X})$ is $\mathrm{B} \to \bar{\mathrm{p}}\mathrm{e}^{+}\nu\mathrm{X}$.

[28] ALEPH Collab., D. Buskulic et al., Phys. Lett. **B 384** (1996) 449;
DELPHI Collab., P. Abreu et al., Z. Phys. **C 68** (1995) 541.

[29] W. Kwong and J.L. Rosner, Phys. Rev. **D 44** (1991) 212.

[30] Personal communications with I.I. Bigi, B. Melic, M. Neubert and M.B. Voloshin.

[31] OPAL Collab., R. Akers et al., Z. Phys. **C 67** (1995) 379.

[32] The LEP Collaborations, ALEPH, DELPHI, L3 and OPAL, and the LEP Electroweak Working Group, Nucl. Inst. and Meth. **A 378** (1996) 101.

[33] ALEPH Collab., D. Buskulic et al., Phys. Lett. **B 365** (1996) 437.